



A Sinc Rule for the Hankel Transform

Eleonora Denich¹ · Paolo Novati¹

Received: 4 January 2024 / Revised: 11 April 2024 / Accepted: 15 May 2024
© The Author(s) 2024

Abstract

This paper deals with the computation of the Hankel transform by means of the sinc rule applied after a special exponential transformation. An error analysis, particularly suitable for meromorphic functions, together with the parameter selection strategy, is considered. A prototype algorithm for automatic integration is also presented.

Keywords Sinc rule · Single exponential transformation · Hankel transform

Mathematics Subject Classification 65D30 · 65D32

1 Introduction

In this work we consider the computation of the Hankel transform of order ν of a function f , given by

$$H^{(\nu)}(\omega) = \int_0^{+\infty} f(x) J_\nu(\omega x) x dx, \quad (1)$$

where $\omega \in \mathbb{R}$ and J_ν is the Bessel function of the first kind of order ν (see [26] for an overview). For $\nu > -\frac{1}{2}$, the inverse Hankel transform is defined as

$$f(x) = \int_0^{+\infty} H^{(\nu)}(\omega) J_\nu(\omega x) \omega d\omega. \quad (2)$$

Sufficient conditions for the validity of (1) and (2) are (see [23]):

1. $f(x) = \mathcal{O}(x^\alpha)$, with $\alpha < -\frac{3}{2}$, for $x \rightarrow +\infty$;
2. $f'(x)$ is piecewise continuous over each bounded subinterval of $[0, +\infty)$;
3. $f(x)$ is such that

$$f(x) = \lim_{\delta \rightarrow 0^+} \frac{f(x+i\delta) + f(x-i\delta)}{2}, \quad i = \sqrt{-1}.$$

The Hankel transform commonly appears in problems of mathematical physics and applied mathematics, described by equations having axial symmetry, as for instance in the analysis

✉ Eleonora Denich
eleonora.denich@phd.units.it

¹ Dipartimento di Matematica e Geoscienze, Università di Trieste, Via Valerio 12/b, 34127 Trieste, Italy

of central potential scattering [24], in geophysical electromagnetic survey [25] and medical tomography [14]. Among the existing techniques employed to compute integral (1), here we quote the ones based on the logarithmic change of variables leading to the Fast Hankel transforms [6, 10, 15], digital filtering algorithms [12, 13, 27], asymptotic expansion of the Bessel function [5, 22], integral representations of the Bessel function [4] and complex Gaussian quadrature [2, 28]. Recently, in [7] a Gaussian rule for weight functions involving powers, exponentials and Bessel functions of the first kind was developed.

In this work we consider the sinc rule together with the single exponential transform

$$x = \frac{\tau}{\omega} \phi(t - q), \quad \phi(\xi) = \frac{\xi}{1 - e^{-\xi}}, \quad (3)$$

where $\tau > 0$ and $q \in \mathbb{R}$ are suitable parameters. The idea is similar to the one developed in [18–21] for Fourier type integrals. In these papers a double exponential approach is considered and an exponential convergence is shown (see also [8]) by a suitable choice of the step size that allows to overcome the difficulties due to the oscillations. Indeed, for Fourier type integrals, the transformations can be defined in order that the quadrature points double exponentially converge to the zeros of the sine/cosine function. This allows to "rapidly" neglect the tails of the sinc rule and then obtain fast convergence. Working with the Hankel transform, the problem is more complicated. Indeed, the double exponential transformations designed for Fourier type integrals do not work properly. The reason is that the zeros of the Bessel function can only be approximated and then a double exponential convergence to them is not achievable. This is the main motivation for the choice of a single exponential transformation of type (3).

In this work we provide a rather accurate error analysis of the truncated sinc rule which shows that, after a proper definition of the step size and the number of points to consider, the error decay is asymptotically quite similar to the one of $f(m)$, for slowly decaying functions, where m is the total number of points of the quadrature rule. If f decays exponentially, then the error is of type $e^{-const\sqrt{m}}$. By exploiting some experimental evidences, we also provide an algorithm for automatic integration in which the only inputs are the function f and the error tolerance. A simple Matlab code is also reported in Appendix.

Throughout the paper, together with $\nu > -\frac{1}{2}$, we always also assume $\nu \neq \frac{1}{2}$, since

$$J_{\frac{1}{2}}(z) = \left(\frac{2}{\pi z}\right)^{\frac{1}{2}} \sin z,$$

(see [17, 10.16.1]), and so integral (1) reduces to a sine transform.

In this work the symbol \sim denotes the asymptotic equality, \approx a generic approximation and \lesssim states for less than or asymptotically equal to.

The paper is organized as follows. In Sect. 2 we recall some basic results concerning the sinc rule over unbounded intervals. In Sect. 3 we study the transformation (3). In Sect. 4 we present the error analysis and in Sect. 5 we show some numerical experiments. In Sect. 6 we describe a prototype automatic integrator, implemented in the Matlab code reported in Appendix.

2 General Results for the Sinc Rule

Before presenting our approach for the Hankel transform, in this section we recall some useful results concerning the sinc approximation

$$I(g) = \int_{-\infty}^{+\infty} g(x)dx \approx h \sum_{j=-\infty}^{+\infty} g(jh), \tag{4}$$

in which $g: \mathbb{R} \rightarrow \mathbb{R}$ is a generic integrable function and h is a positive scalar. Given M and N positive integers, we denote the truncated rule by

$$T_{M,N,h}(g) = h \sum_{j=-M}^N g(jh).$$

Defining the quadrature error as

$$\mathcal{E}_{M,N,h} = |I(g) - T_{M,N,h}(g)|,$$

it holds

$$\mathcal{E}_{M,N,h} \leq \mathcal{E}_D + \mathcal{E}_{T_L} + \mathcal{E}_{T_R},$$

where

$$\mathcal{E}_D = \left| \int_{-\infty}^{+\infty} g(x)dx - h \sum_{j=-\infty}^{+\infty} g(jh) \right|$$

is the discretization error and

$$\mathcal{E}_{T_L} = h \left| \sum_{j=-\infty}^{-M-1} g(jh) \right|, \quad \mathcal{E}_{T_R} = h \left| \sum_{j=N+1}^{+\infty} g(jh) \right|$$

are the truncation errors. For simplicity of notations, we omit their dependence on M, N, h .

Definition 1 [16, Definition 2.12] Given $d > 0$, let \mathcal{D}_d be the infinite strip domain of width $2d$ given by

$$\mathcal{D}_d = \{\zeta \in \mathbb{C}: |\Im(\zeta)| < d\},$$

and let $\mathbf{B}(\mathcal{D}_d)$ be the set of functions analytic in \mathcal{D}_d that satisfy

$$\int_{-d}^d |g(x + i\eta)|d\eta = \mathcal{O}(|x|^a), \quad x \rightarrow \pm\infty, \quad 0 \leq a < 1,$$

and

$$\mathcal{N}(g, d) = \lim_{\eta \rightarrow d^-} \left\{ \int_{-\infty}^{+\infty} |g(x + i\eta)|dx + \int_{-\infty}^{+\infty} |g(x - i\eta)|dx \right\} < +\infty.$$

As for the discretization error, the following theorem holds (see [16, Theorem 2.20]).

Theorem 1 Assume $g \in \mathbf{B}(\mathcal{D}_d)$. Then

$$\mathcal{E}_D \leq \frac{\mathcal{N}(g, d)}{2 \sinh(\pi d/h)} e^{-\frac{\pi d}{h}}. \tag{5}$$

By (5) we have that

$$\mathcal{E}_D \sim \mathcal{N}(g, d)e^{-\frac{2\pi d}{h}}, \quad h \rightarrow 0.$$

The above result shows that, in order to obtain a sharp estimate for \mathcal{E}_D , one should optimize the bound with respect to d , taking into account the position of the singularities of g with respect to \mathcal{D}_d .

In the case of meromorphic functions, the analysis is simpler because one can exploit the results presented in [3, 9], that are based on the use of the residue theorem. Indeed, assuming that the poles of g are simple and symmetric with respect to the real axis, it can be seen that

$$\mathcal{E}_D \sim 4\pi |\rho_0| e^{-2d\frac{\pi}{h}}, \quad h \rightarrow 0, \tag{6}$$

where $\rho_0 = \text{Res}(g(z), z_0)$, $d = |\Im(z_0)|$ and z_0 , together with its conjugate \bar{z}_0 , is the pole closest to the real axis (see also [8] for details). In case of unsymmetric poles, multiplicity greater than one, many poles at the same distance from the real axis, the analysis follows the same line and formula (6) remains true with the factor 4 replaced by another suitable integer as consequence of the residue theorem. Formula (6) is also valid for any function not necessary meromorphic but analytic in a strip symmetric with respect to the real axis, except for two simple poles z_0 and \bar{z}_0 . With respect to the bound (5), the above formula shows an error constant that is independent of d , and a faster exponential decay (in (5) one has to take $d < |\Im(z_0)|$).

3 Exponential Transformation

As mentioned in Introduction, in order to numerically evaluate integral (1), we consider the transformation (3)

$$x = \frac{\tau}{\omega}\phi(t - q), \quad \phi(\xi) = \frac{\xi}{1 - e^{-\xi}}, \tag{7}$$

where $\tau > 0$ and $q \in \mathbb{R}$ are given parameters. We observe that $\phi(\xi) > 0, \forall \xi \in \mathbb{R}, \xi \neq 0$, and

$$\phi(\xi) \sim \begin{cases} |\xi|e^\xi, & \xi \rightarrow -\infty \\ \xi, & \xi \rightarrow +\infty \end{cases}. \tag{8}$$

As for its derivative

$$\phi'(\xi) = \frac{1 - e^{-\xi}(1 + \xi)}{(1 - e^{-\xi})^2},$$

we have that $\phi'(\xi) > 0, \forall \xi \in \mathbb{R}, \xi \neq 0$, and

$$\phi'(\xi) \sim 1, \quad \text{for } \xi \rightarrow +\infty. \tag{9}$$

Remark 1 It is interesting to notice that the function ϕ is the generating function of the Bernoulli numbers B_n ($B_1 = \frac{1}{2}$) [17, 24.2(i)]. Indeed, it holds

$$\phi(\xi) = \sum_{n=0}^{\infty} \frac{B_n \xi^n}{n!},$$

so that the singularities of ϕ and its derivatives at zero can be removed by taking

$$\phi^{(k)}(0) = B_k, \quad k = 0, 1, \dots$$

By using (7), integral (1) becomes

$$H^{(v)}(\omega) = \left(\frac{\tau}{\omega}\right)^2 \int_{-\infty}^{+\infty} \tilde{f}(t) J_\nu(\tau\phi(t-q))\phi(t-q)\phi'(t-q)dt, \tag{10}$$

where $\tilde{f}(t) = f\left(\frac{\tau}{\omega}\phi(t-q)\right)$, and the sinc rule with mesh size h reads

$$H_{M,N,h}^{(v)}(\omega) = \left(\frac{\tau}{\omega}\right)^2 h \sum_{j=-M}^N \tilde{f}(jh) J_\nu(\tau\phi(jh-q))\phi(jh-q)\phi'(jh-q). \tag{11}$$

The term $\phi\phi'$ in (10) introduces a first limitation in the admissible value of d in formula (5) or (6). Indeed, ϕ and ϕ' have a removable singularity at 0 (cf. Remark 1), but they have poles at $2k\pi i, k \in \mathbb{Z}, k \neq 0$. Besides, in order to study the accuracy of (11), it is fundamental to understand how the region of analyticity of f is mapped in the t -plane for \tilde{f} .

To this purpose, let A be the region of analyticity of f ($\mathbb{R}^+ \subset A$) and let $S = \mathbb{C} \setminus A$. In order to study the region of analyticity of \tilde{f} , for any given $w \in S$ we have to find t that solves

$$\frac{\tau}{\omega}\phi(t-q) = w. \tag{12}$$

This reduces to study the equation

$$\phi(\xi) = \frac{\xi}{1 - e^{-\xi}} = z \notin \mathbb{R}^+, \tag{13}$$

whose countable set of solutions is given by

$$\chi(z) = \{\xi \in \mathbb{C} \setminus \{0\} \mid \xi = z + W_k(-ze^{-z}), k \in \mathbb{Z}\},$$

where W_k denotes the k -th branch of the Lambert- W function (see [17, 4.13]). We remark that, even if $\forall z \in \mathbb{C}$ there exists $k \in \mathbb{Z}$ such that

$$z + W_k(-ze^{-z}) = 0, \tag{14}$$

$0 \notin \chi(z)$ because it is not a solution of (13), since $\phi(0) = 1$ (cf. Remark 1). The regions of the complex plane where (14) holds true are reported in [17, Figure 4.13.2].

In order to exploit (5) or (6), we need to study the imaginary part of the set $\chi(\tilde{S})$, where

$$\tilde{S} = \left\{z \in \mathbb{C} \mid z = \frac{\omega}{\tau}w, w \in S\right\},$$

cf. (12). To this purpose, for $z \notin \mathbb{R}^+$, we define the function

$$\Phi(z) = \min |\Im(\chi(z))|. \tag{15}$$

By setting

$$\tilde{d} = \inf_{z \in \tilde{S}} \Phi(z), \tag{16}$$

if \tilde{d} is an isolated minimum, then we can use (6) with $d = \tilde{d}$, otherwise we use (5) with $d < \tilde{d}$. Since in a given subset of the complex plane the function Φ may be defined by using

more than one branch of the Lambert- W function (see again [17, 4.13]), the analysis is not immediate. Anyway, numerically we observe that

$$\Phi(z) \geq \min(\pi, \max(|\arg(z)|, |\Im(z)|)). \tag{17}$$

The above relation can be explained by the following results.

- (a) For any $\frac{\pi}{2} \leq \theta \leq \pi$ and $-\pi \leq \theta \leq -\frac{\pi}{2}$, the function $\Phi(re^{i\theta})$ is increasing with respect to r and $\Phi(re^{i\theta}) \rightarrow 2\pi$ for $r \rightarrow +\infty$. For $0 < \theta < \frac{\pi}{2}$ or $-\frac{\pi}{2} < \theta < 0$, the function $\Phi(re^{i\theta})$ initially increases, reaches a maximum greater than 2π and then tends to 2π . In any case, $\Phi(re^{i\theta}) \rightarrow |\theta|$, for $r \rightarrow 0^+$. Indeed, for $r \rightarrow 0^+$, $\Phi(re^{i\theta})$ involves only W_1 (for $0 < \theta \leq \pi$) or W_{-1} (for $-\pi \leq \theta < 0$) and therefore (cf. (15))

$$\Phi(re^{i\theta}) = \left| \Im \left(re^{i\theta} + W_{\pm 1} \left(-re^{i\theta} e^{-re^{i\theta}} \right) \right) \right|.$$

By using the approximation (see [17, 4.3.11])

$$W_{\pm 1}(-ze^{-z}) = \ln(ze^{-z}) - \ln(-\ln(ze^{-z})) + \mathcal{O}\left(\frac{\ln(-\ln(ze^{-z}))}{\ln(ze^{-z})}\right),$$

with $z = re^{i\theta}$, we obtain

$$\begin{aligned} \Phi(re^{i\theta}) &= \left| r \sin \theta + \Im \left(W_{\pm 1} \left(-re^{i\theta} e^{-re^{i\theta}} \right) \right) \right| \\ &= \pm \theta + \mathcal{O}\left(\frac{1}{\ln r}\right). \end{aligned}$$

- (b) For $0 < y \leq 2\pi$, we have $\Phi(x + iy) \rightarrow y$, for $x \rightarrow +\infty$. This holds true because in this case the branch to consider is W_0 and $W_0(z) \sim z$ for $z \rightarrow 0$ (see [17, 4.13.5]). Moreover, $\Phi(x + iy) \rightarrow 2\pi$, for $x \rightarrow -\infty$, since $\Im(W_k(z)) \rightarrow 2\pi k$, $k \in \mathbb{Z}$, for $|z| \rightarrow \infty$. In particular, for $0 \leq y \leq \pi$, $\Phi(x + iy)$ is monotone increasing. For $\pi < y < 2\pi$, $\Phi(x + iy)$ involves only W_0 and shows a local minimum at $x^* > 0$ where $\pi \leq \Phi(x^* + iy) < y$. Indeed, suppose $\Phi(x^* + iy) < \pi$, then there exists $x^{**} > x^*$ such that, for $z = x^{**} + i\pi$, $\Im(z + W_0(-ze^{-z})) = \pi$, that is $\Im(W_0(-ze^{-z})) = 0$. This is impossible because $\Im(W_0(-ze^{-z})) = 0$ only for $\Im(-ze^{-z}) = 0$, that is, $\tan \Im(z) = \frac{\Im(z)}{\Re(z)}$ (see [17, 4.13]). For $y > 2\pi$, the situation is even more complicated but, nevertheless, $\Phi(x + iy) \geq \pi$. The case of $y < 0$ is specular.

In order to validate the above considerations, in Fig. 1 we show the contour plot of the function $\Phi(z)$.

The accuracy and the efficiency of the sinc rule (11) are strictly related with the choice of τ, q, h . Similarly to the choice made in [8, 21] for the case of Fourier type integrals, the idea is to set

$$\tau = \frac{\pi}{h} \quad \text{and} \quad q = \frac{\pi}{4\tau}(1 - 2\nu), \tag{18}$$

in order to cancel the dominant term in the asymptotic representation of the Bessel function. Indeed, by using (8), (18) and

$$J_\nu(z) = \sqrt{\frac{2}{\pi z}} \left[\cos\left(z - \frac{1}{2}\nu\pi - \frac{1}{4}\pi\right) + e^{|\Im(z)|} \mathcal{O}\left(\frac{1}{z}\right) \right], \quad |z| \rightarrow +\infty, \tag{19}$$

(see [17, p. 223, 10.7.8]), we have that

$$J_\nu(\tau\phi(jh - q)) \sim J_\nu(\tau(jh - q)) = J_\nu\left(j\pi - \frac{\pi}{4}(1 - 2\nu)\right) = \mathcal{O}\left(j^{-\frac{3}{2}}\right), \quad j \rightarrow +\infty,$$

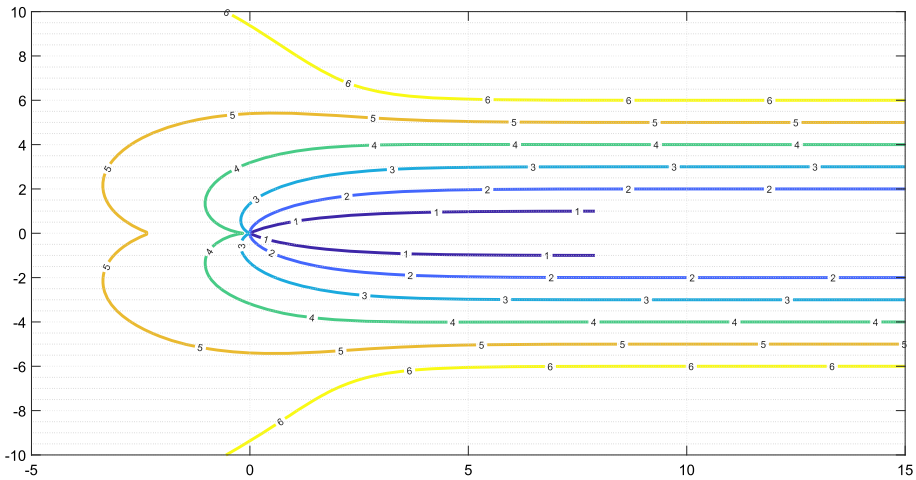


Fig. 1 Contour plot of the function Φ defined in (15)

since

$$\cos\left(\tau(jh - q) - \frac{1}{2}\nu\pi - \frac{1}{4}\pi\right) = \cos\left(j\pi - \frac{\pi}{2}\right) = 0.$$

4 Error Analysis

The analysis presented in this section is based on the standard idea of defining h, M, N in (11) in order to equalize the error contributions $\mathcal{E}_D, \mathcal{E}_{T_L}, \mathcal{E}_{T_R}$. We assume to work with functions f such that

$$f(x) \sim e^{-\beta x^k} x^\alpha, \quad \text{for } x \rightarrow +\infty,$$

with $\beta, k \geq 0, \alpha \in \mathbb{R}$ ($\alpha < -\frac{3}{2}$ if $\beta = 0$ or $k = 0$), and $|f(x)| \leq c$ for $x \in [0, +\infty)$.

4.1 The Discretization Error \mathcal{E}_D

The analysis of the term \mathcal{E}_D has more or less already been given in previous section. Nevertheless, a question still open is how to approximate d in practice. We restrict our considerations to the case of \tilde{d} in (16) isolated minimum. This is true for instance when f is a meromorphic function with poles $\{w_j\}_{j \in J}, J \subseteq \mathbb{Z}$, symmetric with respect to the real axis, and such that $|\Re(w_j)| \leq R, \forall j \in J$, for a certain $R > 0$. Since for $h \rightarrow 0$ ($\tau \rightarrow +\infty$) the set \tilde{S} , now given by

$$\tilde{S} = \left\{ z \in \mathbb{C} \mid z = \frac{\omega}{\tau} w_j, j \in J \right\},$$

tends to collapse on the imaginary axis, we have that $d = \tilde{d} \sim \min_{j \in J} \{|\arg(w_j)|\}$, for $h \rightarrow 0$, since $\Phi(re^{i\theta}) \rightarrow |\theta|$, for $r \rightarrow 0^+$ (see item a) of previous section). Therefore, by

(6),

$$\mathcal{E}_D \sim 4\pi|\tilde{\rho}|e^{-\frac{2\pi d}{h}}, \tag{20}$$

where

$$\tilde{\rho} = \text{Res}(f, \tilde{w})\phi(\tilde{t})J_\nu(\tilde{t})\left(\frac{\tau}{\omega}\right)^2\phi'(\tilde{t}),$$

in which \tilde{w} is the pole of f defining d and \tilde{t} is the corresponding one for \tilde{f} .

4.2 The Truncation Error \mathcal{E}_{T_L}

For the truncation error (see (11))

$$\mathcal{E}_{T_L} = \left| \left(\frac{\tau}{\omega}\right)^2 h \sum_{j=-\infty}^{-M-1} \tilde{f}(jh)J_\nu(\tau\phi(jh-q))\phi(jh-q)\phi'(jh-q) \right|,$$

by using (8)–(9) and the asymptotic relation

$$J_\nu(z) \sim \left(\frac{1}{2z}\right)^\nu \frac{1}{\Gamma(\nu+1)}, \quad z \rightarrow 0, \quad \nu \neq -1, -2, \dots,$$

(see [17, 10,7.3]), where Γ denotes the Gamma function, we have

$$\begin{aligned} \mathcal{E}_{T_L} &\lesssim \left| \frac{c\tau^{\nu+2}}{\omega^2 2^\nu \Gamma(\nu+1)} h \sum_{j=-\infty}^{-M-1} (\phi(jh))^{\nu+1} \phi'(jh) \right| \\ &\lesssim \frac{c\tau^{\nu+2}}{\omega^2 2^\nu \Gamma(\nu+1)} \int_{-\infty}^{-Mh} (\phi(x))^{\nu+1} \phi'(x) dx \\ &\sim \frac{c\pi^{\nu+2}}{\omega^2 2^\nu \Gamma(\nu+1)(\nu+2)} M^{\nu+2} e^{-(\nu+2)Mh}. \end{aligned} \tag{21}$$

4.3 The Truncation Error \mathcal{E}_{T_R}

In order to study the truncation error (see again (11))

$$\mathcal{E}_{T_R} = \left| \left(\frac{\tau}{\omega}\right)^2 h \sum_{j=N+1}^{+\infty} \tilde{f}(jh)J_\nu(\tau\phi(jh-q))\phi(jh-q)\phi'(jh-q) \right|,$$

we first need the following result.

Proposition 1 For $j \rightarrow +\infty$, it holds

$$J_\nu(\tau\phi(jh-q)) = \frac{\sqrt{2}}{8\pi^2} (4\nu^2 - 1) j^{-\frac{3}{2}} (-1)^j \left(1 + \mathcal{O}\left(\frac{1}{j}\right) \right). \tag{22}$$

Proof By writing

$$\begin{aligned} J_\nu(\tau\phi(jh-q)) &= J_\nu(\tau(jh-q)) + J'_\nu(\tau(jh-q))[\tau\phi(jh-q) - \tau(jh-q)] \\ &\quad + \mathcal{O}[\phi(jh-q) - (jh-q)]^2, \end{aligned}$$

and denoting by t_j the j -th positive zero of J_ν , we have

$$\begin{aligned}
 J_\nu(\tau\phi(jh - q)) &= J_\nu(t_j) + J'_\nu(t_j)[\tau(jh - q) - t_j] + \mathcal{O}[\tau(jh - q) - t_j]^2 \\
 &\quad + J'_\nu(\tau(jh - q))(\tau\phi(jh - q) - \tau(jh - q)) \\
 &\quad + \mathcal{O}(\phi(jh - q) - (jh - q))^2.
 \end{aligned}
 \tag{23}$$

At this point, we need the following observations. First of all, for the derivative $J'_\nu(z)$ it holds (see [1, p. 361, 9.1.27])

$$J'_\nu(z) = J_{\nu-1}(z) - \frac{\nu}{2}J_\nu(z),$$

and, in particular,

$$J'_\nu(t_j) = J_{\nu-1}(t_j).
 \tag{24}$$

Moreover, from [1, p. 371, 9.5.12] we have

$$t_j = a_j - \frac{4\nu^2 - 1}{8a_j} + \mathcal{O}\left(\frac{1}{j^2}\right), \quad a_j = \left(j + \frac{1}{2}\nu - \frac{1}{4}\right)\pi.
 \tag{25}$$

Then, remembering that $q = \frac{\pi}{4\tau}(1 - 2\nu)$, $\tau = \frac{\pi}{h}$, and by using (25), we have that

$$\tau(jh - q) - t_j = \frac{4\nu^2 - 1}{8a_j} + \mathcal{O}\left(\frac{1}{j^2}\right).
 \tag{26}$$

Finally, we observe that, for $\xi \rightarrow +\infty$,

$$\tau(\phi(\xi) - \xi) = \tau \frac{\xi e^{-\xi}}{1 - e^{-\xi}} \sim \tau \xi e^{-\xi}.
 \tag{27}$$

By inserting (24)–(26)–(27) in (23), we obtain

$$J_\nu(\tau\phi(jh - q)) = J_{\nu-1}(t_j) \frac{4\nu^2 - 1}{8a_j} + \mathcal{O}\left(\frac{1}{j^2}\right).$$

Now, by using (19) the above expression becomes

$$\begin{aligned}
 J_\nu(\tau\phi(jh - q)) &= \sqrt{\frac{2}{\pi t_j}} \left[\cos\left(t_j - \frac{\nu-1}{2}\pi - \frac{\pi}{4}\right) + \mathcal{O}\left(\frac{1}{t_j}\right) \right] \frac{4\nu^2 - 1}{8a_j} + \mathcal{O}\left(\frac{1}{j^2}\right) \\
 &= \sqrt{\frac{2}{\pi t_j}} \left[(-1)^j + \mathcal{O}\left(\frac{1}{t_j}\right) \right] \frac{4\nu^2 - 1}{8a_j} + \mathcal{O}\left(\frac{1}{j^2}\right),
 \end{aligned}$$

where we have also used (cf. (25))

$$t_j = \left(j + \frac{1}{2}\nu - \frac{1}{4}\right)\pi + \mathcal{O}\left(\frac{1}{j}\right).$$

Finally, since obviously

$$t_j = j\pi \left(1 + \mathcal{O}\left(\frac{1}{j}\right)\right),$$

we obtain the result. □

By the above proposition and relations (8)–(9), for the truncation error \mathcal{E}_{T_R} it holds

$$\mathcal{E}_{T_R} \sim \frac{\sqrt{2}}{8\omega^2} |4v^2 - 1| \left| \sum_{j=N+1}^{+\infty} f\left(\frac{\pi}{\omega}j\right) (-1)^j j^{-\frac{1}{2}} \right|, \quad N \rightarrow +\infty, \tag{28}$$

where we have also used

$$f\left(\frac{\tau}{\omega}\phi(jh - q)\right) \sim f\left(\frac{\tau}{\omega}jh\right) = f\left(\frac{\pi}{\omega}j\right), \quad j \rightarrow +\infty.$$

Then, we have the following results.

Proposition 2 Let $f(x) \sim e^{-\beta x^k} x^\alpha$, for $x \rightarrow +\infty$, with $\beta \geq 0, k \geq 0, \alpha \in \mathbb{R} (\alpha < -\frac{3}{2}$ if $\beta = 0)$. Let moreover

$$f_j = f\left(\frac{\tau}{\omega}j\right) (-1)^j j^{-\frac{1}{2}}. \tag{29}$$

Then,

$$\sum_{j=N+1}^{+\infty} f_j \sim \gamma (-1)^{N+1} \int_N^{+\infty} p(x) dx, \quad N \rightarrow +\infty,$$

where $\gamma = \frac{1}{2} \left(\frac{\pi}{\omega}\right)^\alpha$, and

$$p(x) = e^{-\bar{\beta}x^k} x^{\alpha-\frac{1}{2}} \left(1 - e^{-\bar{\beta}kx^{k-1}} - \left(\alpha - \frac{1}{2}\right) \frac{1}{x} e^{-\bar{\beta}kx^{k-1}}\right), \quad \bar{\beta} = \beta \left(\frac{\pi}{\omega}\right)^k. \tag{30}$$

Proof First of all, we show that

$$f_j + f_{j+1} \sim 2\gamma (-1)^j p(j), \quad \text{for } j \rightarrow +\infty. \tag{31}$$

Since $f(x) \sim e^{-\beta x^k} x^\alpha$, for $x \rightarrow +\infty$, by (29) we have that

$$f_j \sim 2\gamma (-1)^j j^{\alpha-\frac{1}{2}} e^{-\bar{\beta}j^k}, \quad j \rightarrow +\infty.$$

Therefore,

$$f_j + f_{j+1} = 2\gamma (-1)^j e^{-\bar{\beta}j^k} \left(j^{\alpha-\frac{1}{2}} - (j+1)^{\alpha-\frac{1}{2}} e^{-\bar{\beta}((j+1)^k - j^k)}\right).$$

Now, since for $j \rightarrow +\infty$

$$\begin{aligned} (j+1)^k - j^k &\sim kj^{k-1}, \\ (j+1)^{\alpha-\frac{1}{2}} &\sim j^{\alpha-\frac{1}{2}} \left(1 + \left(\alpha - \frac{1}{2}\right) \frac{1}{j}\right), \end{aligned}$$

we obtain (31). Then,

$$\begin{aligned} \sum_{j=N+1}^{+\infty} f_j &= (f_{N+1} + f_{N+2}) + (f_{N+3} + f_{N+4}) + \dots \\ &= \gamma (-1)^{N+1} (2p(N+1) + 2p(N+3) + \dots) \\ &\sim \gamma (-1)^{N+1} \int_N^{+\infty} p(x) dx, \quad N \rightarrow +\infty. \end{aligned}$$

□

Before going on, we recall that, by [11, p. 317, 3.381, n. 3 and p. 942, 8.357],

$$\int_u^{+\infty} x^{\tau-1} e^{-\mu x} dx = \mu^{-\tau} \Gamma(\tau, \mu u) \sim \frac{1}{\mu} u^{\tau-1} e^{-\mu u}, \quad u \rightarrow +\infty, \tag{32}$$

where Γ is the incomplete Gamma function (see e.g. [11, 8.35]).

Proposition 3 *Let f be as in Proposition 2. For $N \rightarrow +\infty$, we have*

- (a) $\mathcal{E}_{T_R} \sim \kappa N^{\bar{\alpha}}$, for $\beta = 0$ and $\alpha < -\frac{3}{2}$,
- (b) $\mathcal{E}_{T_R} \sim \frac{\kappa s}{k\bar{\beta}} N^{\bar{\alpha}-k} e^{-\bar{\beta}N^k}$, for $\beta > 0$ and $k > 0$,

where $\kappa = \frac{\pi^\alpha}{\omega^{\alpha+2}} \frac{\sqrt{2}}{16} |4v^2 - 1|$,

$$\bar{\alpha} = \begin{cases} \alpha - \frac{1}{2}, & 0 < k < 1 \text{ or } \beta = 0 \\ \alpha + \frac{1}{2}, & k \geq 1 \end{cases},$$

and

$$s = \begin{cases} |\frac{1}{2} - \alpha|, & 0 < k < 1 \\ 1 - e^{-\bar{\beta}}, & k = 1 \\ 1, & k > 1 \end{cases}.$$

Proof By (28) and Proposition 2, we have

$$\mathcal{E}_{T_R} \sim \kappa \int_N^{+\infty} p(x) dx.$$

For $\beta = 0$ we have $p(x) = (\frac{1}{2} - \alpha) x^{\alpha-\frac{3}{2}}$, and then (a) straightforwardly follows. For $\beta > 0$, by using (30), a simple asymptotic analysis shows that

$$p(x) \sim s x^{\bar{\alpha}-1} e^{-\bar{\beta}x^k}.$$

At this point,

$$\int_N^{+\infty} p(x) dx \sim s \int_N^{+\infty} x^{\bar{\alpha}-1} e^{-\bar{\beta}x^k} dx = \frac{s}{k} \int_{N^k}^{+\infty} e^{-\bar{\beta}y} y^{\frac{\bar{\alpha}}{k}-1} dy,$$

and using (32) we find (b). □

4.4 Definition of h, M, N

As already mentioned, the idea is to define h, M, N such that $\mathcal{E}_D, \mathcal{E}_{T_R}, \mathcal{E}_{T_L}$ have similar asymptotic behavior. By comparing (5) or (6) and (21) we simply impose

$$(v + 2)Mh = \frac{2\pi d}{h},$$

so that, for any given M , we define

$$h := \sqrt{\frac{2\pi d}{M(v + 2)}}. \tag{33}$$

Then, by inserting (33) in (21), we have

$$\mathcal{E}_{T_L} \sim \frac{c\pi^{\nu+2}}{\omega^2 2^\nu \Gamma(\nu+1)(\nu+2)} M^{\nu+2} e^{-\sqrt{2\pi(\nu+2)dM}}. \tag{34}$$

As for the definition of N , we need to distinguish between the two cases (cf. Proposition 3), that is, we define N by solving

$$\frac{c\pi^{\nu+2} M^{\nu+2} e^{-\sqrt{2\pi(\nu+2) \arg(z_0)M}}}{\omega^2 2^\nu \Gamma(\nu+1)(\nu+2)} = \begin{cases} k N^{\alpha-\frac{1}{2}} & \text{for } \beta = 0, \alpha < -\frac{3}{2} \\ \frac{\kappa s}{k\bar{\beta}} N^{\bar{\alpha}-k} e^{-\bar{\beta}N^k} & \text{for } \beta > 0, k > 0 \end{cases}. \tag{35}$$

We remark that for $\beta = 0$ or $k \approx 0$ previous formulas lead to $N > M$ and, therefore, the error decay with respect to $m = M + N + 1$ is qualitatively given by (a) of Proposition 3 (with N replaced by m). The same holds true for high frequency, since $\bar{\beta}$ may be very small (cf. (30) and (b) of Proposition 3). In these situations, by solving (35), one can observe that $N \approx \omega^{\frac{2\alpha}{2\alpha-1}}$, which represents the deterioration of speed in presence of high frequencies. On the other side, for $\beta > 0$ and $k > \frac{1}{2}$ we obtain $N < M$ and the decay rate is of type $e^{-const\sqrt{m}}$. These considerations are quite evident by looking at Tables 1, 2, 3, 4 and 5 of Sect. 6.

5 Numerical Experiments

In this section we show some numerical experiments in which we compare the sinc rule (11) and the error estimate obtained by summing up the three contributions, that is, $\mathcal{E}_D + \mathcal{E}_{T_L} + \mathcal{E}_{T_R}$, by using (20), (34) and Proposition 3. In particular, for $M = 1, 2, \dots$, we define h as in (33) and N by solving (35). Since the functions considered are

$$\begin{aligned} f_1(x) &= \frac{1}{1+x^2}, \quad \text{with poles } w_j = (-1)^j i, \quad j = 0, 1, \\ f_2(x) &= \frac{x^\nu}{(1+x^4)^{\nu+\frac{1}{2}}}, \quad \text{with poles } w_j = e^{i\frac{\pi}{4}(1+2j)}, \quad j = 0, 1, 2, 3, \\ f_3(x) &= \frac{e^{-x}}{1+x^2}, \quad \text{with poles } w_j = (-1)^j i, \quad j = 0, 1, \\ f_4(x) &= \frac{e^{-x^2}}{1+x^2}, \quad \text{with poles } w_j = (-1)^j i, \quad j = 0, 1, \end{aligned}$$

we use formula (20) with the approximations $d \sim \frac{\pi}{2}$ for f_1, f_3, f_4 and $d \sim \frac{\pi}{4}$ for f_2 .

In Figs. 2, 3, 4 and 5, for different values of ω , we plot the error (obtained with respect to a reference solution), together with the error estimate, with respect to m , the total number of function evaluations.

In this section we also compare formula (11) with the sinc rule applied after using in integral (1) the standard logarithmic change of variables (see e.g. [15])

$$y = \ln\left(\frac{1}{x}\right) \quad \text{and} \quad \lambda = \ln \omega,$$

that leads to

$$H^{(\nu)}(e^\lambda) = \int_{-\infty}^{+\infty} f(e^{-y}) J_\nu(e^{\lambda-y}) e^{-2y} dy. \tag{36}$$

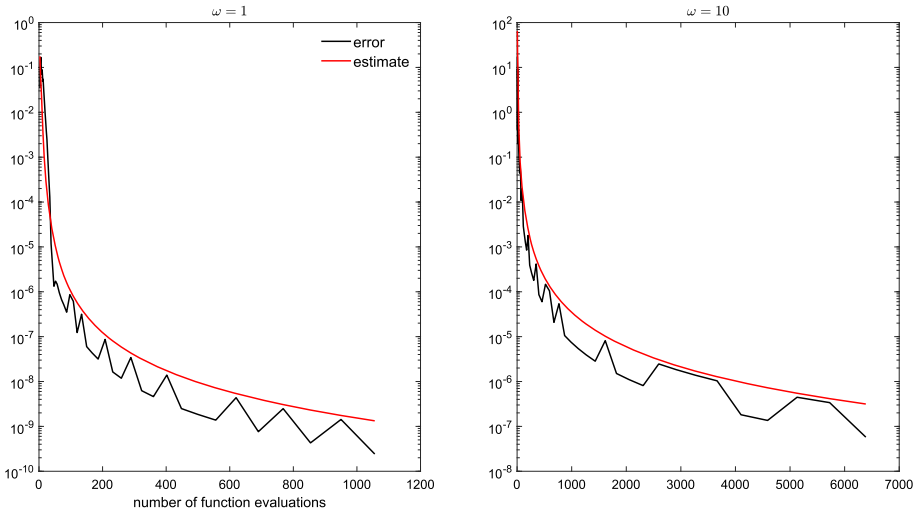


Fig. 2 The error of the sinc rule and the estimate for $f_1(x)$ and $\nu = 0$

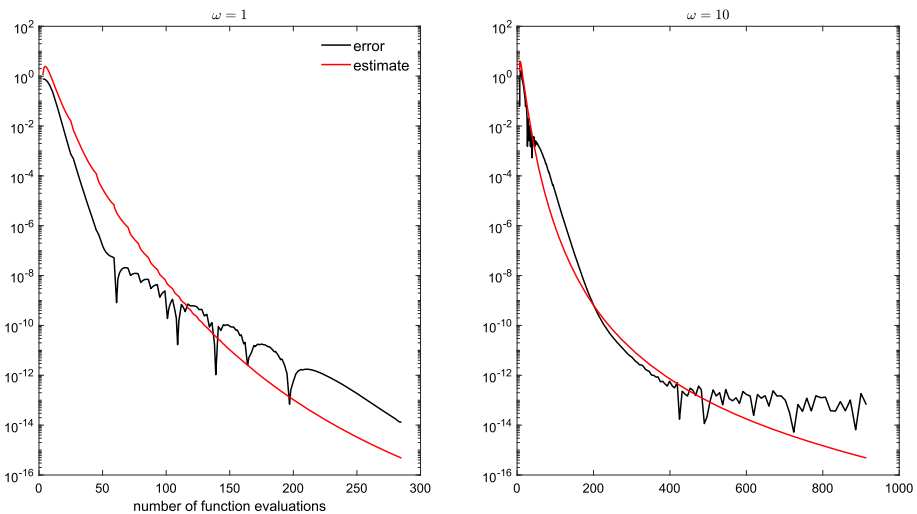


Fig. 3 The error of the sinc rule and the estimate for $f_2(x)$ and $\nu = \frac{3}{2}$

In Fig. 6, working with $f_3(x)$ and $\omega = 1, 5$, we show the results of formula (11) and the ones of the sinc rule applied to (36), with parameters $M = N, h = 1e - 1$ (for $\omega = 1$) and $h = 5e - 2$ (for $\omega = 5$). With respect to the sinc rule applied to (36), this and many other experiments not reported reveal that the sinc rule based on the exponential transformation described in Sect. 3 provides better results, especially for "large" frequencies. Indeed, by increasing ω the problem becomes more difficult due to the oscillations introduced by the Bessel function. By using formula (11), this issue is partially smoothed by the choice made for the parameters of the transformation ϕ (cf. (18)). We remark that we report only the results of a couple of experiments obtained by working with the function $f_3(x)$, which decays

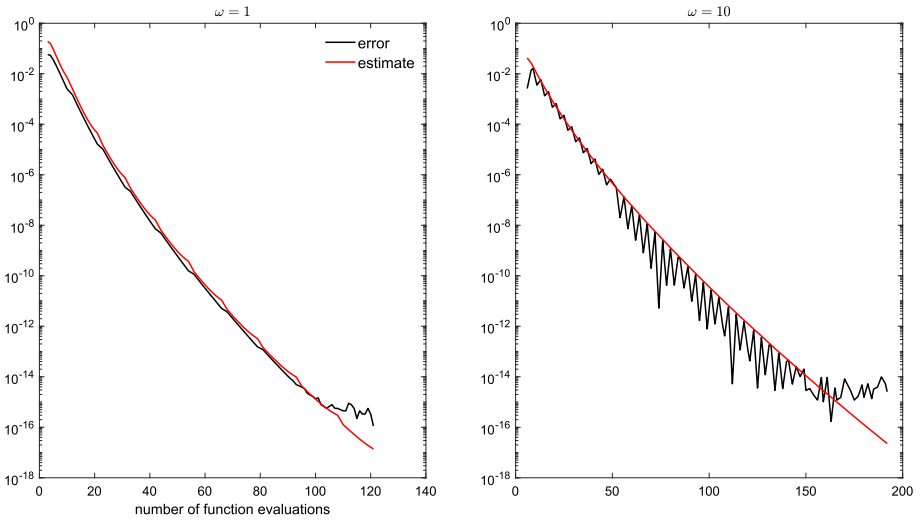


Fig. 4 The error of the sinc rule and the estimate for $f_3(x)$ and $\nu = 1$

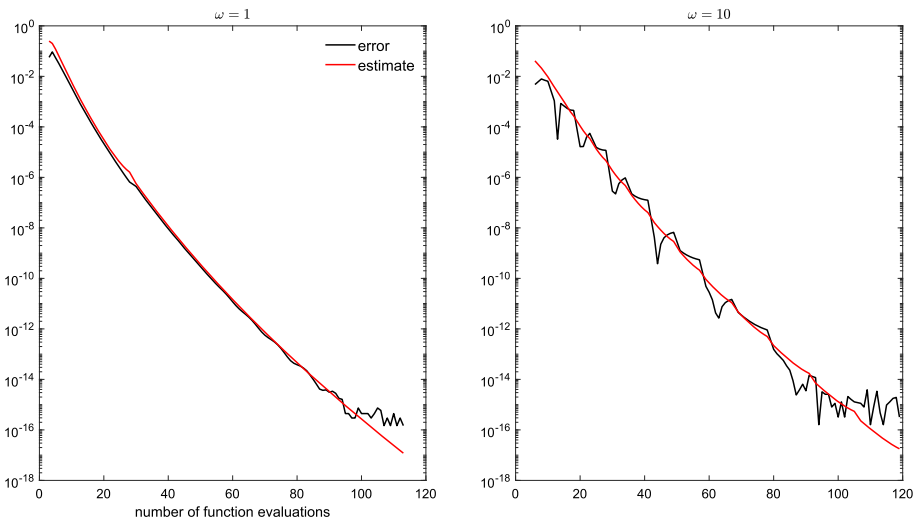


Fig. 5 The error of the sinc rule and the estimate for $f_4(x)$ and $\nu = 0$

exponentially. Indeed, the standard logarithmic change of variable is not suitable for slowly decaying functions.

6 Automatic Integrator

In this section we provide a prototype automatic integrator for the computation of the Hankel transform. The idea is based on the observation that the left truncation error \mathcal{E}_{T_L} does not depend on the function f . Therefore, if for a generic function we plot the total error with

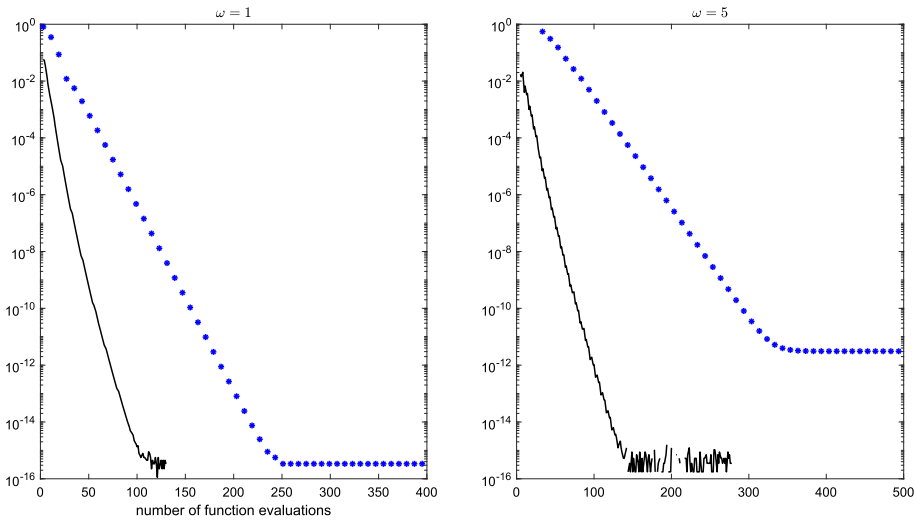


Fig. 6 The relative error of the sinc rule (11) (solid black line) and of the sinc rule applied to integral (36) (blue dots) for $f_3(x)$ and $\nu = 0$ (Color figure online)

respect to M , we always obtain something of the type

$$\mathcal{E}_{M,N,h} \approx \gamma 10^{-\delta M},$$

with $\gamma, \delta > 0$. By running a number of experiments with different functions we have observed that conservative but rather good values of the parameters are given by

$$\delta = \frac{1}{5} \quad \text{and} \quad \gamma = 1.$$

In this way, by setting an arbitrary tolerance η , the idea is to define

$$M = -5 \log_{10} \eta.$$

Then, in order to define h , we impose (cf. (21))

$$\frac{\pi^{\nu+2}}{\omega^2 2^\nu \Gamma(\nu+1)(\nu+2)} M^{\nu+2} e^{-(\nu+2)Mh} = \eta,$$

that leads to

$$h = \frac{1}{(\nu+2)M} \left(\ln \frac{M^{\nu+2}}{\eta} + \ln \frac{\pi^{\nu+2}}{\omega^2 2^\nu \Gamma(\nu+1)(\nu+2)} \right). \tag{37}$$

As for the choice of N , we observe that

$$\mathcal{E}_{T_R} \sim c_{\omega,\nu} f\left(\frac{\pi}{\omega} N\right) N^{-\frac{1}{2}},$$

with $c_{\omega,\nu} = \frac{\sqrt{2}}{16} \omega^2 |4\nu^2 - 1|$ (cf. Proposition 3). Then, we set N as the numerical solution of

$$c_{\omega,\nu} f\left(\frac{\pi}{\omega} N\right) N^{-\frac{1}{2}} = \eta. \tag{38}$$

We summarize the above strategy in the following algorithm.

Table 1 Results of Algorithm 2 with $f(x) = e^{-x}$, $\nu = 0$

| | | $\eta = 1e - 4$ | $\eta = 1e - 7$ | $\eta = 1e - 10$ |
|---------------|-------|-----------------|-----------------|------------------|
| $\omega = 1$ | Error | $5.6e - 5$ | $6.3e - 8$ | $8.9e - 11$ |
| | M | 20 | 35 | 50 |
| | N | 5 | 5 | 7 |
| | h | 0.42 | 0.35 | 0.32 |
| | k | 1 | 1 | 5 |
| $\omega = 5$ | Error | $2.8e - 4$ | $1.8e - 5$ | $2.5e - 9$ |
| | M | 20 | 35 | 50 |
| | N | 5 | 14 | 25 |
| | h | 0.34 | 0.31 | 0.29 |
| | k | 1 | 10 | 20 |
| $\omega = 20$ | Error | $3.3e - 3$ | $5.4e - 7$ | $6.6e - 11$ |
| | M | 20 | 35 | 50 |
| | N | 5 | 36 | 77 |
| | h | 0.27 | 0.27 | 0.26 |
| | k | 1 | 10 | 20 |

Algorithm 2 Given $\eta > 0$

1. set $M = \lceil -5 \log_{10} \eta \rceil$;
2. set h as in (37);
3. solve problem (38) to define N ;
4. evaluate integral (1) by using (11).

In Tables 1, 2, 3, 4 and 5, working with different functions and taking $\omega = 1, 5, 20$, we report the results of Algorithm 2 for $\eta = 1e - 4, 1e - 7, 1e - 10$. In particular, we solve problem (38) by employing the secant method with $N_0 = 5$ as starting point. In the tables we also report the number of iterations of the secant method, denoted by k , since it represents an additional number of function evaluations. As stopping criteria for the secant algorithm we set a termination tolerance in the order of η and a maximum number of iterations $k_{\max} = 100$. The Matlab code that implements Algorithm 2 is reported in Appendix. We want to point out that the code can be labeled as a first attempt. For instance, the subfunction relative to the secant method is not optimized and can be strongly improved. Nevertheless, a further development would also be the computation on a vector of frequencies.

7 Conclusion

In this work we have considered the computation of the Hankel transform of a function f by employing a particular exponential transformation followed by the sinc rule. A rather accurate error analysis, based on the theory of analytic functions, allowed to properly define the parameters of the quadrature formula and to derive quite sharp error estimates. The theory and the numerical experiments reveal that the rule is also able to handle the difficult cases represented by the presence of slowly decaying functions f . The main reason is that the choice of the parameters of the exponential transform and, as consequence, of the step size allowed to manage the oscillations due to the Bessel function, especially for increasing frequency. Anyway, for increasing values of ω the method slows down (cf. Sect. 4.4). The

Table 2 Results of Algorithm 2

with $f(x) = \frac{\ln(1+x)}{1+x^3}$, $\nu = 1$

| | | $\eta = 1e - 4$ | $\eta = 1e - 7$ | $\eta = 1e - 10$ |
|---------------|-------|-----------------|-----------------|------------------|
| $\omega = 1$ | Error | $1.4e - 5$ | $3.6e - 7$ | $1.7e - 10$ |
| | M | 20 | 35 | 50 |
| | N | 5 | 36 | 275 |
| | h | 0.33 | 0.27 | 0.24 |
| | k | 1 | 12 | 23 |
| $\omega = 5$ | Error | $1.9e - 3$ | $2.2e - 7$ | $1.4e - 10$ |
| | M | 20 | 35 | 50 |
| | N | 6 | 50 | 431 |
| | h | 0.28 | 0.24 | 0.22 |
| | k | 2 | 13 | 25 |
| $\omega = 20$ | Error | $7.8e - 4$ | $1.5e - 7$ | $1.8e - 10$ |
| | M | 20 | 35 | 50 |
| | N | 5 | 70 | 571 |
| | h | 0.23 | 0.21 | 0.20 |
| | k | 1 | 12 | 23 |

Table 3 Results of Algorithm 2

with $f(x) = e^{-\frac{1}{2}x^{\frac{3}{2}}}$, $\nu = 2$

| | | $\eta = 1e - 4$ | $\eta = 1e - 7$ | $\eta = 1e - 10$ |
|---------------|-------|-----------------|-----------------|------------------|
| $\omega = 1$ | Error | $1.2e - 4$ | $1.2e - 7$ | $1.2e - 10$ |
| | M | 20 | 35 | 50 |
| | N | 5 | 5 | 5 |
| | h | 0.28 | 0.22 | 0.20 |
| | k | 1 | 1 | 1 |
| $\omega = 5$ | Error | $1.4e - 4$ | $1.8e - 7$ | $3.9e - 11$ |
| | M | 20 | 35 | 50 |
| | N | 8 | 13 | 18 |
| | h | 0.24 | 0.20 | 0.18 |
| | k | 5 | 14 | 24 |
| $\omega = 20$ | Error | $2.4e - 3$ | $6.3e - 7$ | $1.9e - 11$ |
| | M | 20 | 35 | 50 |
| | N | 15 | 41 | 62 |
| | h | 0.20 | 0.18 | 0.17 |
| | k | 4 | 14 | 24 |

prototype automatic integrator, implemented in Matlab, has been successfully tested on several examples and, in our opinion, it represents a good starting point for the development of a reliable code.

Table 4 Results of Algorithm 2

with $f(x) = e^{-\sqrt{x}} \ln(1+x)$,
 $\nu = \frac{3}{2}$

| | | $\eta = 1e-4$ | $\eta = 1e-7$ | $\eta = 1e-10$ |
|---------------|-------|---------------|---------------|----------------|
| $\omega = 1$ | Error | $5.3e-4$ | $1.3e-7$ | $1.7e-10$ |
| | M | 20 | 35 | 50 |
| | N | 23 | 71 | 146 |
| | h | 0.30 | 0.24 | 0.22 |
| | k | 9 | 19 | 29 |
| $\omega = 5$ | Error | $5.2e-4$ | $1.5e-7$ | $1.7e-10$ |
| | M | 20 | 35 | 50 |
| | N | 32 | 195 | 491 |
| | h | 0.26 | 0.22 | 0.20 |
| | k | 6 | 17 | 27 |
| $\omega = 20$ | Error | $5.2e-3$ | $1.9e-7$ | $1.5e-10$ |
| | M | 20 | 35 | 50 |
| | N | 17 | 365 | 1308 |
| | h | 0.22 | 0.20 | 0.19 |
| | k | 2 | 12 | 23 |

Table 5 Results of Algorithm 2

with $f(x) = \frac{x}{\cosh x}$, $\nu = 2$

| | | $\eta = 1e-4$ | $\eta = 1e-7$ | $\eta = 1e-10$ |
|---------------|-------|---------------|---------------|----------------|
| $\omega = 1$ | Error | $2.4e-5$ | $4.2e-9$ | $7.1e-13$ |
| | M | 20 | 35 | 50 |
| | N | 5 | 7 | 9 |
| | h | 0.28 | 0.22 | 0.20 |
| | k | 1 | 3 | 14 |
| $\omega = 5$ | Error | $8.1e-4$ | $7.5e-7$ | $4.7e-10$ |
| | M | 20 | 35 | 50 |
| | N | 12 | 24 | 35 |
| | h | 0.24 | 0.20 | 0.18 |
| | k | 7 | 17 | 27 |
| $\omega = 20$ | Error | $7.0e-6$ | $1.1e-7$ | $1.1e-10$ |
| | M | 20 | 35 | 50 |
| | N | 53 | 71 | 116 |
| | h | 0.20 | 0.18 | 0.17 |
| | k | 2 | 6 | 16 |

Matlab code

```

1 function [H,nval] = Hankel(f,w,ni,eta)
2 % HANKEL evaluates the Hankel transform H^(ni)(w)
  (see (1))
3 % with prescribed error tolerance around eta. The
  code
4 % follows the steps of Algorithm 7.

```

```

5 % In output nval is the total number of function
  evaluations
6
7 % step 1
8 M = ceil(-5*log10(eta));
9 % step 2
10 K = pi^(ni+2)/(w^2*2^ni*gamma(ni+1)*(ni+2));
11 h = 1/((ni+2)*M)*log(K*M^(ni+2)/eta);
12 % step 3
13 c = sqrt(2)/16/(w^2)*abs(4*ni^2-1);
14 fun = @(x) c*f(pi/w*x).*x.^(-1/2);
15 [N,k] = secant(fun,eta); N = ceil(N);
16 % step 4
17 phi = @(t) t./(1-exp(-t));
18 phiP = @(t) (1-exp(-t)-t.*exp(-t))./(1-exp(-t))
  .^2;
19 v = [-M:N]*h;
20 tau = pi/h; q = pi/(4*tau)*(1-2*ni);
21 F = @(t) f(tau/w.*phi(t-q)).*(tau/w)^2.*phi(t-q).*
  ...
  besselj(ni,tau*phi(t-q)).*phiP(t-q);
22 % output
24 H = h*sum(F(v)); nval = M+N+1+k;
25
26     function [N,k] = secant(fun,eta)
27         N0 = 5; N = N0; N1 = N0+1; st = 1; kmax =
100;
28         F0 = fun(N); F1 = fun(N1); k = 1;
29         while st > eta && k < kmax && abs(F1) >=
eta
30             der = (F1-F0)/(N1-N0);
31             if der >= 0
32                 disp('solution not found, increase
N0')
33                 break
34             end
35             N = N - (F1-eta)/der;
36             N0 = N1; F0 = F1;
37             N1 = N; F1 = fun(N);
38             st = abs(F1-eta);
39             k = k+1;
40         end
41     end
42
43 end

```

Acknowledgements This work was partially supported by GNCS-INdAM and FRA-University of Trieste. The authors are member of the INdAM research group GNCS. Eleonora Denich thanks the University of Trieste for the support, under grant “Programma Regionale (PR) FSE+ 2021/2027 della Regione Autonoma

Friuli Venezia Giulia - PPO 2023 - Programma specifico 22/23 - Avviso emanato con decreto n.17895/GRFVG dd.19.04.2023 s.m.i., Linea C) Sportello 2023”.

Funding Open access funding provided by Università degli Studi di Trieste within the CRUI-CARE Agreement.

Data Availability Enquiries about data availability should be directed to the authors.

Declaration

Conflict of interest The authors declare that they have no conflict of interest.

Open Access This article is licensed under a Creative Commons Attribution 4.0 International License, which permits use, sharing, adaptation, distribution and reproduction in any medium or format, as long as you give appropriate credit to the original author(s) and the source, provide a link to the Creative Commons licence, and indicate if changes were made. The images or other third party material in this article are included in the article's Creative Commons licence, unless indicated otherwise in a credit line to the material. If material is not included in the article's Creative Commons licence and your intended use is not permitted by statutory regulation or exceeds the permitted use, you will need to obtain permission directly from the copyright holder. To view a copy of this licence, visit <http://creativecommons.org/licenses/by/4.0/>.

References

1. Abramowitz, M., Stegun, I.A.: Handbook of Mathematical Functions with Formulas, Graphs, and Mathematical Tables. Dover Books on Intermediate and Advanced Mathematics, 7th edn. Dover Publications Inc., New York (1970)
2. Asheim, A., Huybrechs, D.: Complex Gaussian quadrature for oscillatory integral transforms. *IMA J. Numer. Anal.* **33**(4), 1322–1341 (2013)
3. Barrett, W.: Convergence properties of Gaussian quadrature formulae. *Comput. J.* **3**, 272–277 (1960/1961)
4. Candel, S.: An algorithm for the Fourier–Bessel transform. *Comput. Phys. Commun.* **23**(4), 343–353 (1981)
5. Candel, S.M.: Dual algorithms for fast calculation of the Fourier-Bessel transform. *IEEE Trans. Acoust. Speech Signal Process.* **29**, 963–972 (1981)
6. Christensen Niels, B.: Optimized fast Hankel transform filters. *Geophys. Prospect.* **38**(5), 545–568 (1990)
7. Denich, E., Novati, P.: Gaussian rule for integrals involving Bessel functions. *BIT Numer. Math.* **63**(4), 53 (2023)
8. Denich, E., Novati, P.: Some notes on the trapezoidal rule for Fourier type integrals. *Appl. Numer. Math.* **198**, 160–175 (2024)
9. Donaldson, J.D., Elliott, D.: A unified approach to quadrature rules with asymptotic estimates of their remainders. *SIAM J. Numer. Anal.* **9**(4), 573–602 (1972)
10. Ghosh, D.P.: The application of linear filter theory to the direct interpretation of geoelectrical resistivity sounding measurements. *Geophys. Prospect.* **19**(2), 192–217 (1971)
11. Gradshteyn, I.S., Ryzhik, I.M.: Table of Integrals, Series, and Products, 4th edn. Academic Press, New York (1980)
12. Guptasarma, D.: Optimization of short digital linear filters for increased accuracy. *Geophys. Prospect.* **30**(4), 501–514 (1982)
13. Guptasarma, D., Singh, B.: New digital linear filters for Hankel j_0 and j_1 transforms. *Geophys. Prospect.* **45**(5), 745–762 (1997)
14. Higgins, W.E., Munson, D.C.: A Hankel transform approach to tomographic image reconstruction. *IEEE Trans. Med. Imaging* **7**(1), 59–72 (1988)
15. Johansen, H.K., Sorensen, K.: Fast Hankel transforms. *Geophys. Prospect.* **27**, 876–901 (1979)
16. Lund, J., Bowers, K.L.: Sinc Methods for Quadrature and Differential Equations. Society for Industrial and Applied Mathematics (1992)
17. Olver, F., Lozier, D., Boisvert, R., Clark, C.: The NIST Handbook of Mathematical Functions. Cambridge University Press, New York (2010)
18. Oura, T.: A double exponential formula for the Fourier transforms. *Publ. Res. Inst. Math. Sci.* **41**(4), 971–977 (2005)

19. Ooura, T., Mori, M.: The double exponential formula for oscillatory functions over the half infinite interval. *J. Comput. Appl. Math.* **38**(1), 353–360 (1991)
20. Ooura, T., Mori, M.: Double exponential formula for Fourier type integrals with a divergent integrand, pp. 301–308 (1993)
21. Ooura, T., Mori, M.: A robust double exponential formula for Fourier-type integrals. *J. Comput. Appl. Math.* **112**, 229–241 (1999)
22. Oppenheim, A.V., Frisk, G.V., Martinez, D.R.: Computation of the Hankel transform using projections. *J. Acoust. Soc. Am.* **68**(2), 523–529 (1980)
23. Piessens, R.: *The Hankel Transforms*, Chap. 9. CRC Press LLC, Boca Raton (2000)
24. Sharafeddin, O.A., Ferrel Bowen, H., Kouri, D.J., Hoffman, D.K.: Numerical evaluation of spherical Bessel transforms via fast Fourier transforms. *J. Comput. Phys.* **100**(2), 294–296 (1992)
25. Ward, S.H., Hohmann, G.W.: 4. *Electromagnetic Theory for Geophysical Applications*, pp. 130–311 (2012)
26. Watson, G.N.: *A treatise on the theory of Bessel functions*, 2nd reprinted edn. Cambridge University Press (1966)
27. Werthmüller, D., Key, K., Slob, E.C.: A tool for designing digital filters for the Hankel and Fourier transforms in potential, diffusive, and wavefield modeling. *Geophysics* **84**(2), F47–F56 (2019)
28. Wong, R.: Quadrature formulas for oscillatory integral transforms. *Numer. Math.* **39**, 351–360 (1982)

Publisher's Note Springer Nature remains neutral with regard to jurisdictional claims in published maps and institutional affiliations.